Improving the throwing power of acidic zinc sulfate electroplating baths

Magdy AM Ibrahim*
Chemistry Department, Faculty of Science, Ain Shams University, Abbassia, Cairo, Egypt

Abstract: The effect of some plating parameters, such as Zn^{2+} ion concentration, pH, current density, temperature and duration on the throwing power, as well as on the throwing index of acidic zinc sulfate baths has been investigated. The addition of *p*-anisidine (PA) and/or sodium dodecylbenzenesulfonate (DBS) has been examined as a possible means of improving the uniformity of deposit distribution. The additives cause a substantial increase in the overpotential for the reduction of Zn^{2+} ions and consequently improve the throwing power of the baths. The throwing power increases by a factor of four in the presence of DBS and a factor of one-and-a-half in the presence of PA. The inhibition of zinc reduction was assumed to occur via adsorption of the PA or DBS molecules on the cathode surface and the adsorption followed the Langmuir adsorption isotherm. The surface morphology of the zinc plated with and without the additives was examined by using scanning electron microscopy (SEM).

Keywords: throwing power; electroplating; Wagner number; zinc sulfate; Tafel lines; organic additives

1 INTRODUCTION

In electroplating processes it is insufficient to produce deposits having the desired appearance and properties. The coating must be applied in such a way as completely to cover the substrate with a deposit as near uniform in thickness as practicable.[1]

Zinc deposition has been extensively investigated under various operating conditions depending on the applications considered or the aims chosen.[2] Zinc can be electrodeposited from both alkaline and acidic baths.[3–8] Sulfate baths are fairly popular in the electrometallurgy of zinc even though cyanide-containing baths are commonly used for industrial purposes.[2] Cyanide baths have good throwing power, but their toxicity is a serious disadvantage.[3]

Despite the numerous published results relevant to the electrochemistry of zinc deposition from sulfate baths, the study of their throwing power is rare. These baths are known to have a poor throwing power.[3] Only the throwing powers of acidic copper and tin plating baths have been extensively studied.[9–15]

Adding organic compounds is one of the most effective and most frequently used methods to improve both the quality of the deposits and the throwing power of electrolytic baths.[16] The organic additives usually contain polarizable or charged groups, almost always based on N- or S-containing groups, eg amines, proteins and alkaloids, sulfonates, mercaptans and sulfides. Moreover, surfactants are widely used in the electroplating industry to prevent formation of acidic mist by hydrogen evolution at the cathode.[17]

Therefore, the aim of the present study is to investigate the influence of some plating parameters as well as the influence of PA and/or DBS on the throwing power and throwing index of zinc from acidic sulfate baths.

2 EXPERIMENTAL DETAILS

Reagent grade *p*-anisidine (PA) and sodium dodecylbenzenesulfonate (DBS) (anionic surfactant) were used without further purification. The PA solution was prepared by dissolving the appropriate amount in $1\,cm^3$ ethanol (pa Merck), then added to the electrolyte. All solutions were prepared using bidistilled water. The pH of the electrolyte was adjusted by addition of 1:1 H_2SO_4. For electrodeposition runs, a steel cathode and a platinum sheet anode, each of dimensions $2.5\,cm \times 3.0\,cm$ were used. The plating cell used for the efficiency measurements was a rectangular Perspex trough ($10\,cm \times 3.0\,cm$) provided with vertical grooves machined on each of the side walls to fix the electrodes. Before each run, the steel cathode was mechanically polished with different grade emery papers, 600, 800, 1000 and 1500 meshes, and then washed with distilled water, rinsed with ethanol and weighed. Plating current was supplied by a dc power supply (model GPS-3030D). The cathodic current efficiencies, ϕ, were determined with the help of a Cu-coulometer ($\phi = Wt_{exp}/Wt_{theo}$) where Wt_{exp} is the weight of the deposit obtained experimentally and Wt_{theo} is the weight of the deposit calculated by

* Correspondence to: Magdy AM Ibrahim, Materials and Structures Lab, Tokyo Institute of Technology, 4259 Nagatsuta, Midori, Yokohama, 226-8503, Japan
E-mail: mag1@rlem.titech.ac.jp
(*Received 18 November 1999; revised version received 4 April 2000; accepted 6 April 2000*)

Faraday's law. All the experiments were carried out using unstirred solutions and the duration of plating was 10 min. Most of the experiments were carried out at 25 ± 2 °C.

The throwing power (TP) of the solution was measured using a Haring–Blum rectangular Perspex cell (3.0 cm wide, 13.0 cm long, with 2.5 cm solution depth) fitted with one anode between two parallel cathodes where the ratio of the far to the near distance was 5:1. The percentage throwing power was calculated from Field's formula:[18]

$$TP\% = \frac{L - M}{L + M - 2} \times 100$$

where L is the current distribution ratio or linear ratio (5:1) and M is the metal distribution ratio of the near to the far cathodes.

The values of M were measured as a function of L over a wide range of linear ratios varying between 1:1 and 5:1. The throwing index (TI) of each bath was considered as the reciprocal of the slope of the M versus L plot.[19]

Potentiodynamic cathodic polarization measurements were performed in the rectangular cell. A potentiostat/galvanostat (EG&G model 273) controlled by a Personal Computer was used for the potentiodynamic measurements. All potentials were measured relative to a saturated calomel electrode (SCE). To avoid contamination, the reference electrode was connected to the working steel cathode via a bridge provided with a Luggin–Haber tip and filled with the solution under test. The tip was pressed against the electrode surface.

The surface morphology of the zinc electrodeposits was examined using scanning electron microscopy (JEOL-JEM 1200 EX II electron microscope).

3 RESULTS AND DISCUSSION

3.1 Potentiodynamic cathodic polarization curves and Tafel lines

Cathodic polarization is an important factor with respect to the throwing power of a bath, because together with the ohmic resistance, it determines the distribution of the plating current and, consequently, the metal distribution over various parts of the cathode.[20] Therefore, the potentiodynamic cathodic polarization curves for zinc electrodeposition were measured under different plating conditions. The curves were swept from the rest potential (about −0.8 V) up to −1.6 vs SCE at a scan rate of 10 mV s^{-1}. Examples of these curves are given in Figs 1–5. The data reveal that, in general, the deposition of zinc from these solutions is accompanied by a large polarization. Simultaneous discharge of hydrogen ions was observed during the deposition of the Zn^{2+} ions. Inspection of the data in Fig 1 shows that increasing

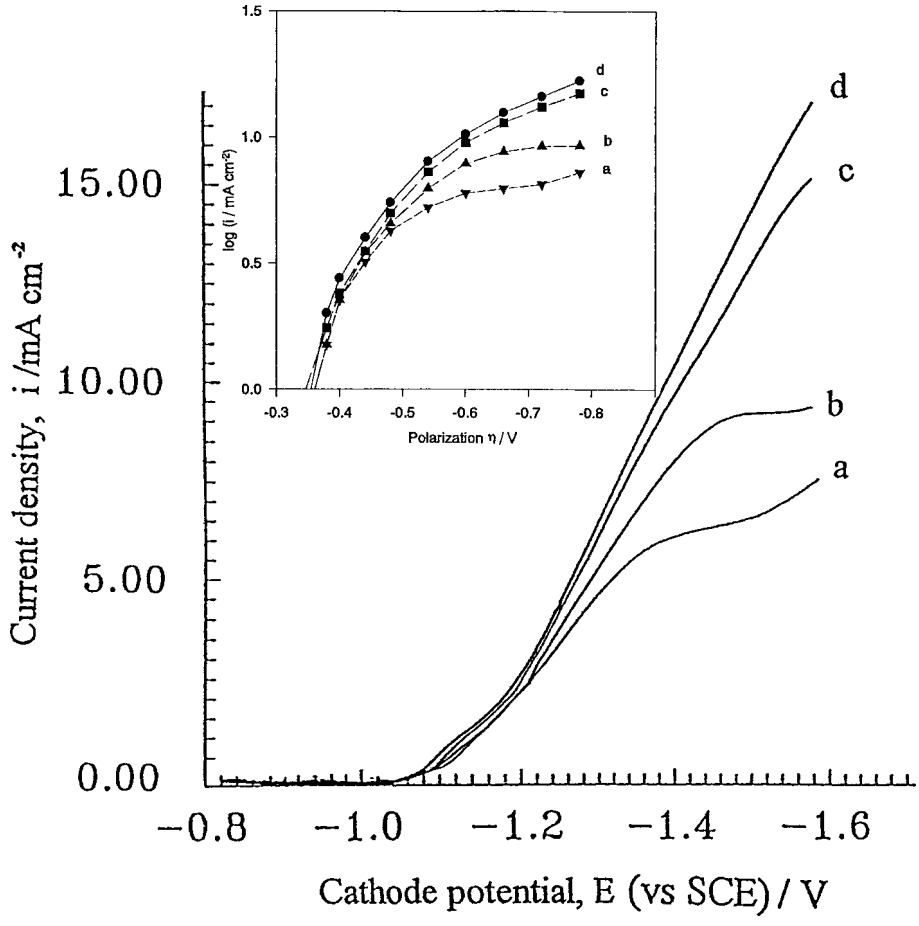

Figure 1. Potentiodynamic cathodic polarization curves and Tafel plots (insert) during zinc electrodeposition; curve (a): 0.09 M $ZnSO_4$ and 0.2 M Na_2SO_4, curve (b): 0.15 M $ZnSO_4$ and 0.2 M Na_2SO_4, curve (c): 0.24 M $ZnSO_4$ and 0.2 M Na_2SO_4 and curve (d): 0.35 M $ZnSO_4$ and 0.2 M Na_2SO_4.

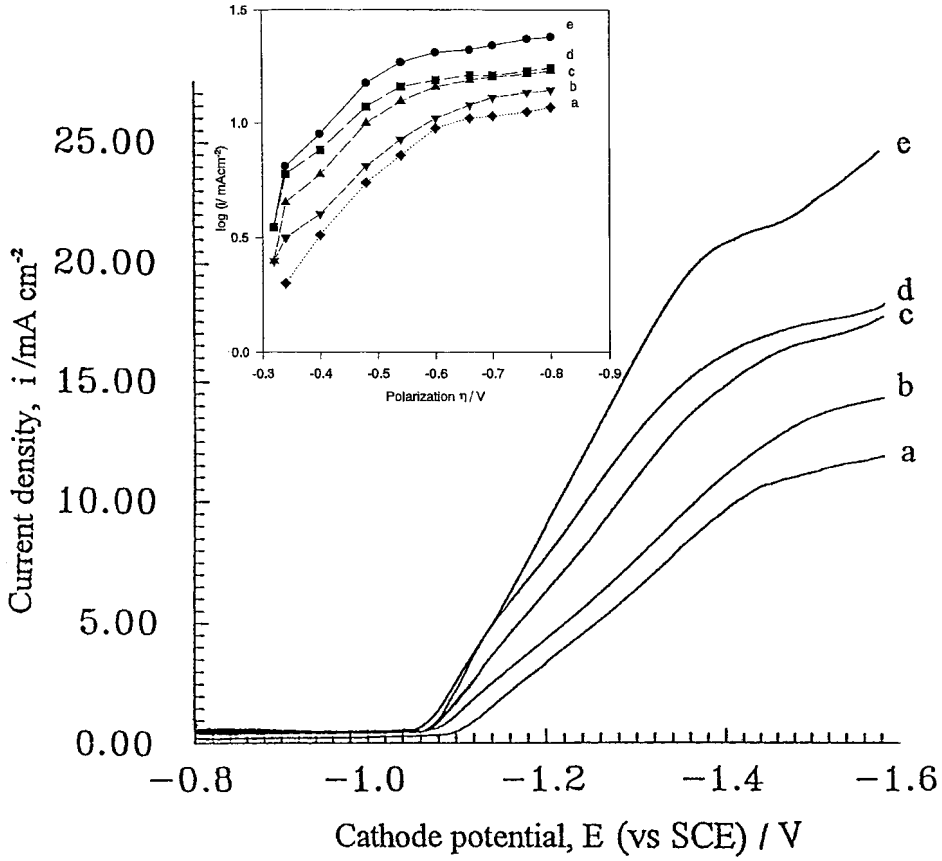

Figure 2. Potentiodynamic cathodic polarization curves and Tafel plots (insert) during zinc electrodeposition from Zn.1 bath at different temperatures; curve (a): $T = 25\,°C$, (b) $T = 40\,°C$, (c) $T = 50\,°C$, (d) $T = 60\,°C$ and curve (e) $T = 70\,°C$.

the Zn^{2+} ions content in the bath shifts the polarization curves towards the less negative potentials. These results can be related to the increase in the relative concentration of Zn^{2+} ions in the diffusion layer and this is reflected in the decrease in concentration polarization which occurs during zinc deposition. Moreover, in the case of deposition from a solution with a low content of Zn^{2+} ions (curves a and b), the current tends to attain a limiting value, which results, at least partially, from the control of deposition caused by the diffusion of Zn^{2+} ions.

The bath selected for further investigations contained 0.15 M $ZnSO_4$, 0.2 M Na_2SO_4 and the pH was adjusted to about 3.2. The selected bath was designated as Zn.1. The effect of pH variation (pH 2.0–5.0) on the cathodic polarization curves showed a decrease of polarization with pH (data not shown).

The effect of temperature (25–70 °C) on the cathodic polarization curves of zinc deposition from the selected bath is shown in Fig 2. The data reveal that the cathodic polarization decreases with increasing temperature. Similar results were obtained as a result of rising bath temperature during electrodeposition of other metals.[6,21,22] This behaviour could be attributed to a decrease of the activation polarization of the reducible species.[23] Moreover, an increase in temperature enhances the concentration of the reducible species in the diffusion layer due to an increased diffusion coefficient.

In an attempt to improve the throwing power of the zinc plating baths, DBS and/or PA were added into plating Zn.1 bath. Figures 3–5 reveal that the electrodeposition of zinc in the presence of these additives occurs by a greater polarization than in the absence of either of them.

Figure 3 gives the cathodic polarization curves for zinc deposition with and without addition of different concentrations of DBS (0.015×10^{-3}–0.15×10^{-3} M). It can be seen that the presence of DBS results in a marked shift in the cathodic polarization towards more negative potential values. At a given potential, it is clear that the current decreases with increasing concentrations of DBS, indicating inhibition of the deposition of Zn^{2+} ions. The inhibitory effect of DBS could be due to its adsorption on the metal surface. On the other hand, similar behaviour was expected by the addition of PA at different concentrations (0.1×10^{-3}––6.0×10^{-3} M) into the plating zinc bath, as shown in Fig 4. PA makes its own contribution to levelling for it is more accessible to the promontories, which protrude further into the electrolyte, and so form a more complete adsorbed layer there which slows down deposition.[24] A combination of DBS and PA causes a greater shift in cathodic polarization than the shift produced from the presence of an individual additive at the same concentration, indicating a larger hindrance of Zn^{2+} ions deposition (see Fig 5).

To clarify the effect of the above variables on the electrode kinetics, Tafel lines are derived from the corresponding *i–E* curves (Figs 1–5) by plotting the

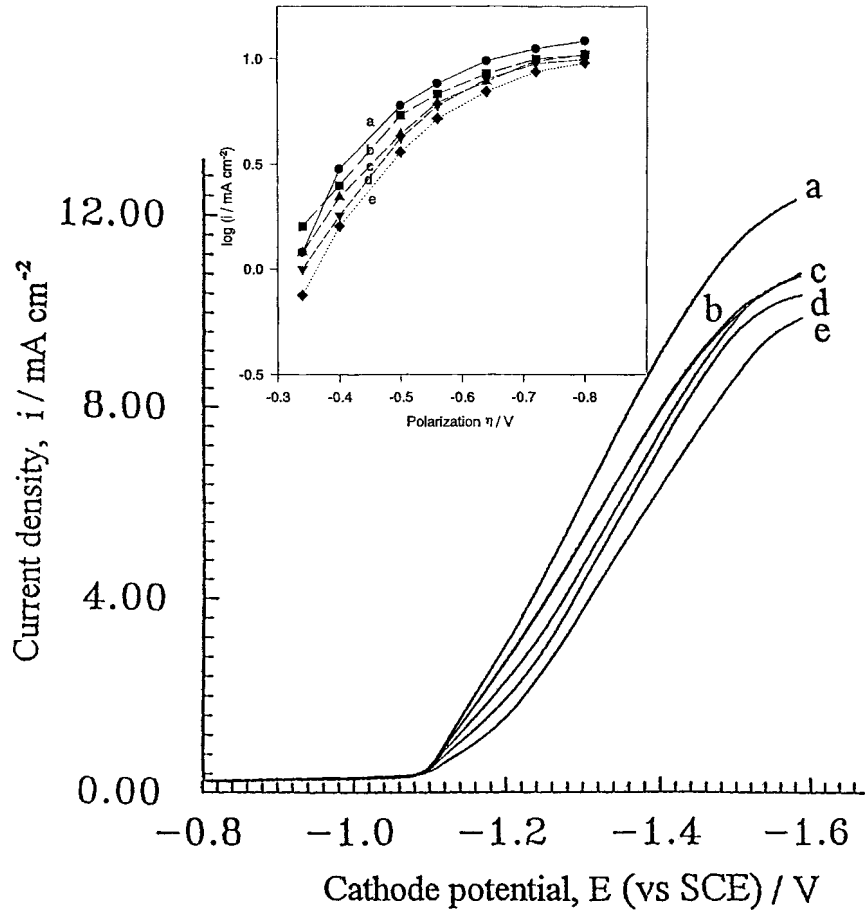

Figure 3. Potentiodynamic cathodic polarization curves and Tafel plots (insert) during zinc electrodeposition from Zn.1 bath in presence of different concentrations of DBS; curve (a) 0.00, (b) 0.015×10^{-3} M, (c) 0.03×10^{-3} M, (d) 0.08×10^{-3} M and curve (e) 0.15×10^{-3} M.

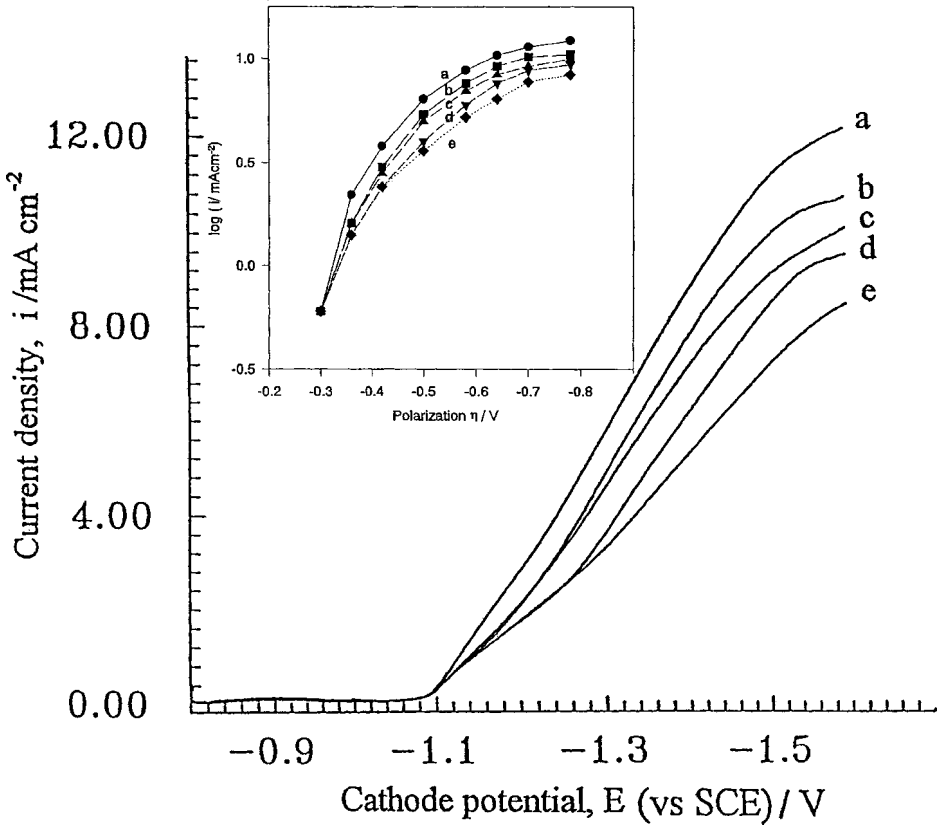

Figure 4. Potentiodynamic cathodic polarization curves and Tafel plots (insert) during zinc electrodeposition from Zn.1 bath in presence of different concentrations of PA; curve (a) 0.00, (b) 0.1×10^{-3} M, (c) 0.3×10^{-3} M, (d) 4.0×10^{-3} M and curve (e) 6.0×10^{-3} M.

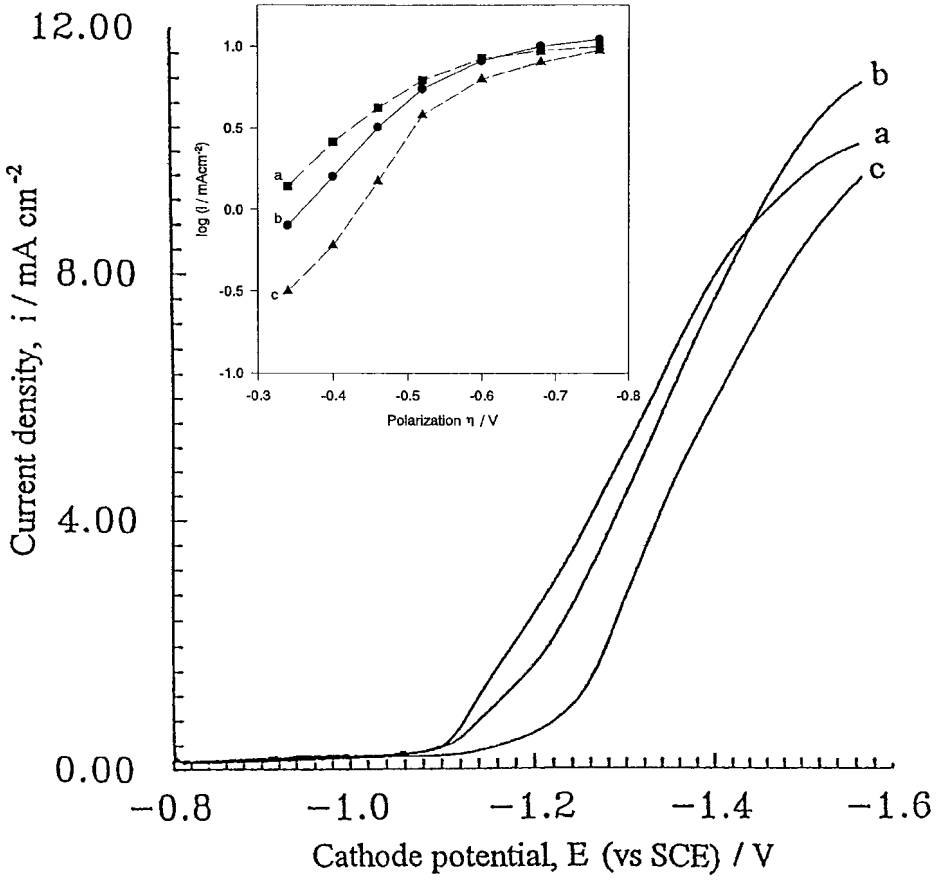

Figure 5. Potentiodynamic cathodic polarization curves and Tafel plots (insert) during zinc electrodeposition from Zn.1 bath; curve (a) 0.08×10^{-3}M DBS, (b) 0.1×10^{-3}M PA, (c) 0.08×10^{-3}M DBS+0.1×10^{-3}M PA.

logarithm of the current vs the cathodic polarization ($\eta = E - E_s$) according to the Tafel equation:

$$\eta = a + b\log i \qquad (1)$$

$$b = RT/\alpha nF$$

where b is the Tafel slope, α is the transfer coefficient and i is the current density. Exchange current densities, i_o, for zinc deposition were obtained by extrapolating the Tafel lines to zero overpotential. The Tafel slopes calculated from the straight lines at high polarization (−0.55 to −0.80V) for different plating solutions as well as the exchange current densities, i_o, and the transfer coefficient, α, are listed in Table 1.

Data in Table 1 show that increasing concentration of Zn^{2+} in the electrolyte has a slight effect on Tafel slopes although i_o is increased with increasing Zn^{2+} ion concentrations, indicating that the charge transfer reaction is not controlled by the concentration of Zn^{2+} ions.[25] However, the effect of temperature on Tafel slopes at high polarization is expected due to the presence of limiting currents in the i–E curves. This means that at high temperature and at high polarization the zinc deposition is a mass transfer-controlled process. Moreover, data in Table 1 indicate that Tafel slopes are markedly decreased in the presence of DBS, especially at low concentrations, while the transfer coefficient, α, is increased with increasing DBS concentrations, implying that the charge transfer reaction was affected strongly by the presence of DBS. This means also that DBS decreases significantly the rate of Zn^{2+} ion transfer across the electrical double layer and partial blocking of active sites is possible. It should be mentioned here that, generally, the charge transfer reactions are responsible for the formation of metallic deposits at the metal–electrolyte interface. However, if

Table 1. Tafel kinetic parameters obtained for different plating solutions at high polarizations (−0.55 to −0.80)

Tafel lines	*Tafel slopes b (mV decade^{-1})*	*Exchange current density log i_o (mA cm^{-2})*	*Transfer coefficient (α)*
Fig 1			
Curve a	56.0	0.0073	3.3
Curve b	68.0	0.0085	4.0
Curve c	69.0	0.0091	4.1
Curve d	65.0	0.0097	3.9
Fig 3			
Curve b	28.0	0.0087	1.7
Curve c	46.0	0.0084	2.7
Curve d	58.0	0.0082	3.4
Curve e	65.0	0.0079	3.9
Fig 4			
Curve b	68.0	0.0087	4.0
Curve c	67.0	0.0084	4.0
Curve d	72.0	0.0082	4.2
Curve e	68.0	0.0074	4.0
Fig 5			
Curve c	44.0	0.0070	2.6

deposit growth is limited by diffusion only, an unstable situation develops, because protruding parts of a surface grow faster, since they are more accessible. Dentritic deposits, or even powder, are produced under these conditions.[25]

On the other hand, Tafel slopes and the transfer coefficient, α, remain nearly constant in the presence of PA at almost all concentrations. However, a combination of the two additives shows that the Tafel slope as well as the transfer coefficient α are decreased markedly, indicating that the charge transfer reactions are controlled by the presence of the two additives. It is worthwhile to mention here that the decrease in the exchange current i_o with increasing DBS or PA concentrations is systematic and is consistent with increased additive adsorption on the cathode. Tripathy *et al*[25] found a similar relationship between the exchange current i_o and the concentration of other additives for zinc deposited from acidic sulfate solutions

3.2 Adsorption isotherms

The additive molecules of DBS and PA are thought to adsorb on the cathode surface. This phenomenon increases the deposition overpotential by decreasing the sites available for discharge of Zn^{2+} ions (see Figs 3–5). Therefore, the surface coverage by the additive can be estimated from eqn (2):

$$\theta = (1 - i_{add}/i) \qquad (2)$$

where i and i_{add} are the current density without and with the additives at a constant potential value (-1.45 V vs SCE). The data are fitted by a Langmuir adsorption isotherm, eqn (3):

$$\theta/(1-\theta) = K[C] \qquad (3)$$

where K is the equilibrium constant of the adsorption reaction and [C] is the additive concentration in the bulk of the solution. Figure 6 gives the results of the Langmuir plots for the adsorption data of the two additives DBS and PA. From the adsorption isotherm shown in Fig 6 the equilibrium constant K was evaluated to be $1.7 \times 10^3\,\text{M}^{-1}$ for DBS and $8.0\,\text{M}^{-1}$ for PA, suggesting a chemical adsorption.[26] A large value of K means higher adsorption of a given compound ie stronger electrical interactions between the double layer existing at the phase boundary and the adsorbing molecules. The standard free energy change (ΔG_a^o) for adsorption was estimated using eqn (4):

$$\Delta G_a^o = -RT \ \ln\,(55.5\,K) \qquad (4)$$

in a similar way as reported for organic molecules[27] where R is the universal gas constant, T is the absolute temperature and 55.5 is the molarity of water. The large value of free energy change of -28.2 kJ mol^{-1} for DBS and -15.0 kJ mol^{-1} for PA confirms the extent of the chemisorption at the metal–solution interface.[28] Also, the large value of ΔG_a^o and its negative sign indicate that the adsorption of DBS or PA on the steel

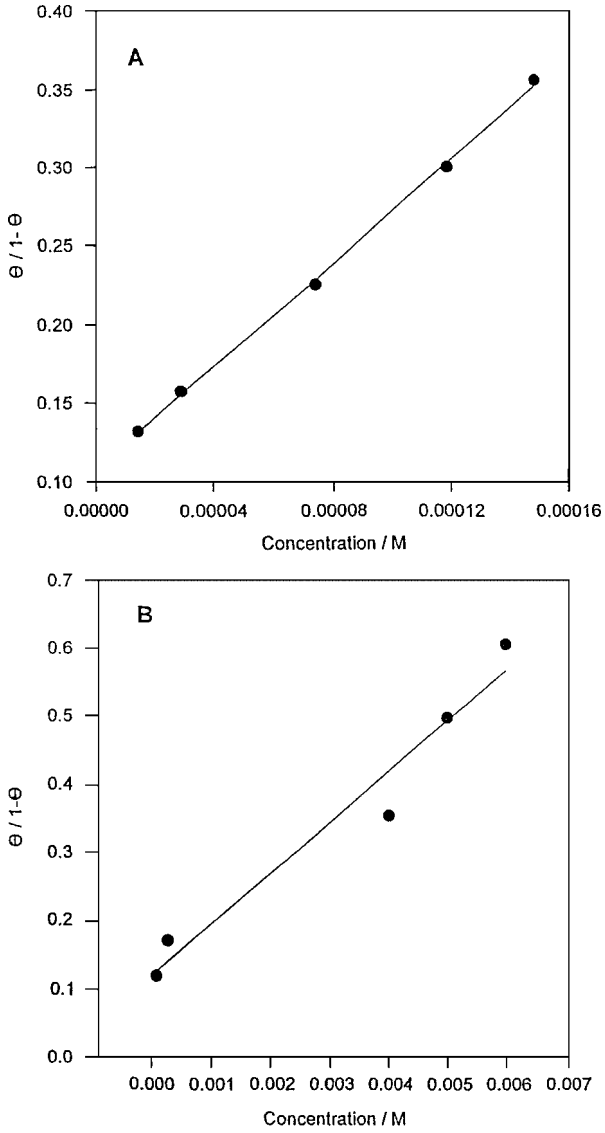

Figure 6. Plot of [θ/(1-θ)] against concentration [C] to evaluate ΔG_a^o; (A) DBS and (B) PA.

surface is proceeding spontaneously and that adsorption is very efficient. Similar value of $\Delta G_a^o = -30.2$ kJ mol^{-1} for DBS was reported[29] as a result of its adsorption on an aluminium surface in an acidic medium.

To illustrate the way by which the adsorption of the additives could occur and its effect on the nucleation process, some basic information must be considered: a DBS molecule is ionized in solution to produce alkyl acid radical negative ions which can easily be adsorbed at the cathode surface with the hydrophilic group facing the cathode and the hydrophobic group facing the liquid medium. Of course, after the surfactant molecule is adsorbed on the cathode surface by the electrostatic force, it may still react with the cathode surface to form the chemical bond. The high values of K and ΔG_a^o indicate this possibility. Since the critical micelle concentration (CMC) of DBS[29] is 1.2×10^{-3} M it means that the DBS concentrations used in this work are below the CMC. This suggests that the

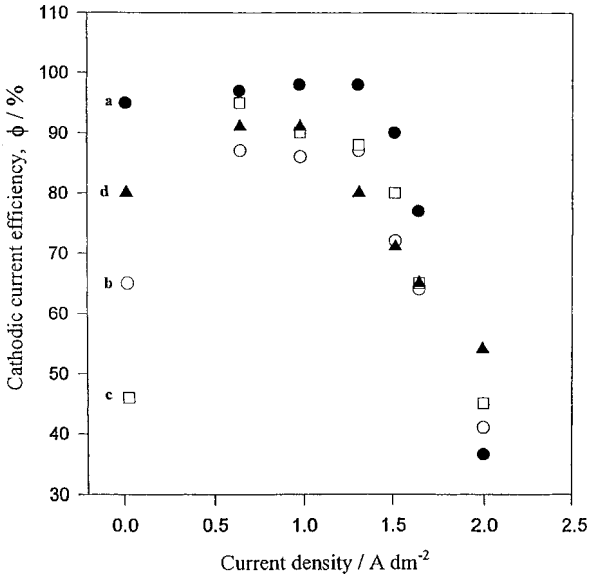

Figure 7. Cathodic current efficiency against current density for zinc electrodepostion from Zn.1 bath: (a) in absence of additives, (b) 0.08×10^{-3} M DBS, (c) 0.1×10^{-3} M PA and (d) 0.1×10^{-3} M PA + 0.08×10^{-3} M DBS.

interaction with the surface is on the monomolecular level since no micelles form at these concentrations.

Generally speaking, the influence of adsorption can be understood by considering its effect on nucleation. Nucleation theory states that the rate of nucleation increases with overpotential. However, DBS would affect the rate of nucleus formation in two different ways: directly, through a blocking of active sites on the substrate which will diminish the nucleation rate and indirectly, by reducing the growth rate of zinc deposition which at constant current will increase the overpotential and the rate of nucleus formation. On the other hand, the extent of adsorption of PA is lower than that of DBS, as is clear from comparing the values of K and ΔG^{o}_{a}. This could probably be explained by the fact that the PA molecule has a small size in comparison with the large size of the DBS molecule. In addition, PA could compete with the adsorbed DBS on the surface.

3.3 Cathodic current efficiency

The effect of the applied current density upon the cathodic current efficiency, $\%\phi$, during zinc electrodeposition in the absence and in the presence of DBS, PA or a combination of them, was studied and the results are shown in Fig 7. Inspection of the data shows that the efficiency is strongly dependent on the current density. The data reveal that the $\%\phi$ in the absence of the additives is high (about 95%) at low current densities (up to $1.3\,A\,dm^{-2}$), then falls to 40% at $2\,A\,dm^{-2}$ as a result of simultaneous hydrogen evolution.[30] Addition of DBS, PA or a combination of them resulted in a decrease in the $\%\phi$.

3.4 Throwing power and throwing index

The throwing power of the acidic sulfate baths was measured using a Haring–Blun cell under variable plating conditions. According to the cell geometry, the total cell current i is divided into two partial currents, i_n and i_f, corresponding to the respective cathodes. In the absence of polarization, the primary current ratio (i_n/i_f) depends on the electrical resistance of the electrolyte between the anode and the respective cathodes, ie it is inversely proportional to the ratio of their distances from the anode. Thus the primary current ratio should be equal to the distance ratio, L. Once the current passes, polarization takes place and it is assumed that it will be higher at the nearer cathode than at the farther one. Because polarization resistance may be considered as being in series with the ohmic resistance, the current at the nearer cathode is decreased, giving rise to a more uniform secondary current distribution ratio. More equalization of the current ratio could be achieved by increasing the conductivity of the bath.

The throwing power values of the zinc sulfate plating baths calculated by Field's empirical formula at a distance ratio of 1:5 under different plating conditions are shown in Table 2 and 3. Inspection of the data in Table 2 shows that the percentage throwing power, TP%, of Zn.1 bath is very low. Increasing the concentration of Zn^{2+} ions in the bath enhances the throwing power although it decreases the polarization curves (see Fig 1). This could be attributed to the increase in the electrolytic conductivity (see Table 2) of the solution with increasing Zn^{2+} ions content. Increasing the electrolytic conductivity results in improved throwing power.[31] On the other hand,

i (A dm^{-2})	Temp (°C)	pH	Time (min)	TP(%)	TI	κ (Ω^{-1} cm^{-1})	(Wa)
1.33	25	3.2	10	−14.9	0.76	0.40	3.2×10^{-3}
1.33[a]	25		10	15.9	1.37	0.47	
1.70	25	3.2	10	14.3	1.33	0.40	
2.70	25	3.2	10	24.0	1.57	0.40	
1.33	40	3.2	10	1.27	1.04	0.41	3.4×10^{-3}
1.33	50	3.2	10	19.0	1.41	0.43	3.8×10^{-3}
1.33	25	2.5	10	−14.9	0.76	0.43	
1.33	25	4.5	10	15.9	1.37	0.40	
1.33	25	3.2	15	9.6	1.22	0.40	

[a] This bath contains 0.35 M $ZnSO_4$ and 0.2 M Na_2SO_4.

Table 2. Effect of some plating parameters on the throwing power (TP%) throwing index (TI), and Wagner number (*Wa*) for zinc electrodeposition from Zn.1 bath

Table 3. Effect of DBS, PA and a combination of them on the TP%, TI and *Wa* for zinc electrodeposition from Zn.1 bath, pH 3.2, $i=1.33\,A\,dm^{-2}$, $t=10$ min at 25 °C

Additives concentration	*TP(%)*	*TI*	*κ* ($\Omega^{-1}cm^{-1}$)	*Wa*
0.00	−14.9	0.76	0.40	3.2×10^{-3}
0.1×10^{-3} M PA	1.3	1.03	0.40	3.4×10^{-3}
2.0×10^{-3} M PA	7.4	1.18	0.40	
0.08×10^{-3} M DBS	31.2	1.96	0.39	4.2×10^{-3}
0.15×10^{-3} M DBS	51.0	3.13	0.37	5.4×10^{-3}
0.1×10^{-3} M PA + 0.08×10^{-3} M DBS	40.4	2.27	0.38	5.0×10^{-3}

increasing the current density improves the throwing power. This could be attributed to the increase in cathodic polarization. Increasing temperature leads to an increase in throwing power and this is due to the increase in the electrical conductivity of the solution (see Table 2). Reducing the pH of bath Zn.1 to 2.5 has no pronounced effect on the throwing power. However, increasing the pH to 4.5 allows the throwing power to be improved. This result is in contradiction with the fact that the electrical conductivity (Table 2) and the cathodic polarization are decreased to some extent with higher solution pH. A similar effect was observed for cobalt electrodeposition from sulfate baths.[32] It is also of interest to notice that increasing duration improves the throwing power (see Table 2).

The effects of adding different concentrations of DBS and PA and a combination of them on the throwing power of Zn.1 bath are given in Table 3. Generally, it is clear that addition of DBS or PA or their combination greatly improves the throwing power. However, addition of DBS has a more pronounced effect on improving throwing power and its value reaches 51% at 0.15×10^{-3} M. This means that for these conditions, the throwing power increases more than four times in comparison with the DBS-free bath. On the other hand, it is increased by one-and-a-half times by the presence of PA. This improvement in throwing power is only dependent on the concentration of the additives added. The increase in throwing power could be attributed to the preferential adsorption of the additives on the cathode surface on particularly active sites, growth at these locations is then blocked for the reduction of Zn^{2+} ions.[28] These results could be confirmed by the shift of polarization curves in a negative direction with increasing concentration of the additives (see Figs 3–5).

Jelinek and David[19] reported that some of the ambiguities associated with the use of the concept of 'throwing power' can be resolved by the use of 'throwing index' which is obtained by plotting the metal distribution ratio M versus the linear current distribution ratio L on arithmetic co-ordinates. The reciprocal of the slope of the line obtained is the throwing index and represents a direct estimate for the bath throwing power. It should be noted that a solution with ideal throwing characteristics would produce a horizontal line at $M=1$, whereas a bath with a poor throwing power would exhibit a very steep line in this plot.

Some representative linear plots between the metal distribution ratio M, and the linear ratio L (1:1–1:5) are given in Figs 8–10. The values of throwing power and throwing index given in Tables 2 and 3 reveal that the calculated values of TI change in a parallel manner to those calculated for TP. Expressing the results in the form of throwing index rather than throwing power is advantageous because five experimental points are taken during the measurements of the throwing index and this minimizes errors in measurement of any one point. In addition, a single number which is characteristic of a range of linear ratios is obtained.

3.5 Wagner number

The degree of electrodeposition uniformity is characterized by the Wagner number,[33,34] *Wa*, which represents the ratio of the electrochemical reaction to the ohmic resistances. The Wagner number is defined by:

$$Wa = (\kappa/x)\cdot(\mathrm{d}\eta/\mathrm{d}i) \qquad (5)$$

where κ is the electrical conductivity of the solution, x is the breadth of the electrode (3.0 cm in this work) and $(\mathrm{d}\eta/\mathrm{d}i)$ is the slope of the potential–current density curve. The Wagner numbers calculated for different solutions are included in Tables 2 and 3. The results

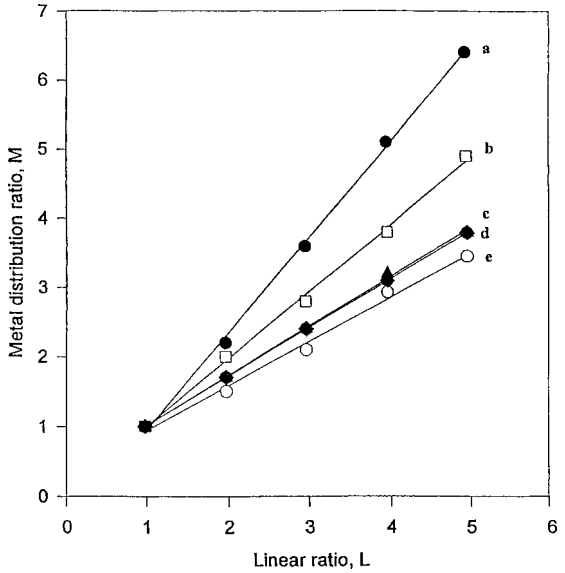

Figure 8. Metal distribution ratio M against linear ratio L. Curve (a): Zn.1 bath, pH 3.2, $i=1.33\,A\,dm^{-2}$, $t=10$ min, $T=25$ °C, curve (b) the same as (a) but $T=40$ °C, curve (c) the same as (a) but $[ZnSO_4]=0.35$ M, curve (d) the same as (a) but $T=50$ °C and curve (e) the same as (a) but $i=2.7\,A\,dm^{-2}$.

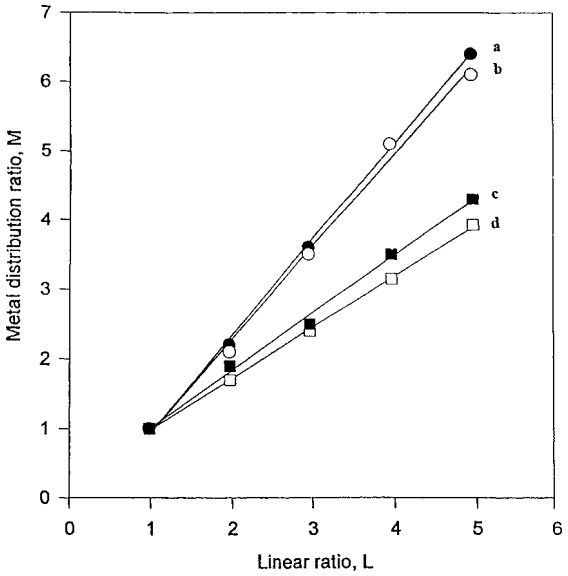

Figure 9. Metal distribution ratio *M* against linear ratio *L* for Zn.1 bath, Curve (a), Zn.1 bath, pH 3.2, $i = 1.33\ A\,dm^{-2}$, $t = 10$ min, $T = 25\,^{\circ}C$, curve (b) the same as (a) but pH 2.4, curve (c) the same as (a) but $t = 15$ min, curve (d) the same as (a) but pH 4.5.

confirm that the current density distribution becomes more uniform as the Wagner number increases. The data of the throwing power, throwing index and Wagner number are in good agreement with each other. The more uniform the current distribution, the higher the Wagner number and consequently the higher the throwing power as well as the throwing index.

3.6 Surface morphology

The surface morphology of the as-plated zinc deposit from Zn.1 bath was examined by SEM. Figure 11 shows the photomicrographs of zinc deposits obtained with (thickness = 3.8 μm) and without additives (thickness = 3.2–3.4 μm). In the absence of the additives, the deposits were not uniform, showing grains of various sizes (Fig 11(a)). In contrast, when the electrolyte contained DBS and/or PA, the deposits obtained were fine-grained, homogeneous and uniform (Fig 11(b–d)). This could be explained by the fact that in the presence of the additives, the electrodeposition of zinc is associated with considerable polarizations (Figs 3–5) which leads to an increase in the nucleation density and consequently a decrease in the grain size of the deposits.[35] The presence of PA induced reticular grains (network structure) of zinc over the whole surface and produced a smaller degree of surface roughness (Fig 11(b)). On the other hand, in the presence of DBS more uniform deposits formed, comprising fine grains with columnar growth in a pyramidal form (Fig 11(c)).

The surface morphology of the zinc electrodeposit from Zn.1 bath including both DBS and PA (Fig 11(d)) passed from a reticular (in the case of PA) or a pyramidal columnar grain (in the case of DBS) to spherical grains of almost equal sizes. The additives not only made the deposits much more finer grained, but also enhanced the uniformity of the surface. This means that these additives have a levelling action.[36]

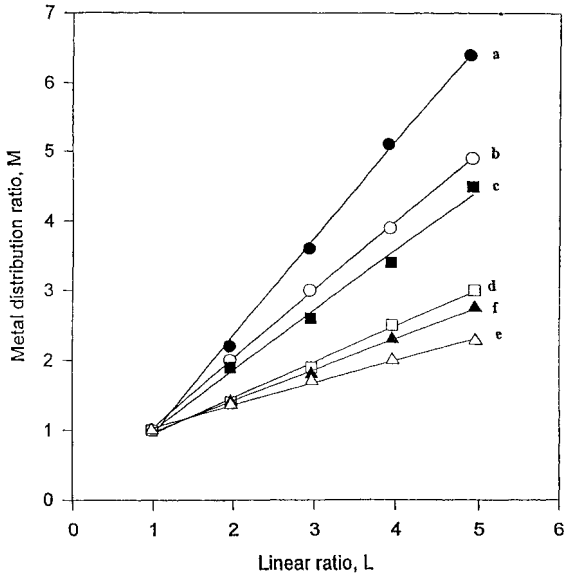

Figure 10. Metal distribution ratio *M* against linear ratio *L*. Curve (a) in absence of additives, (b) 0.1×10^{-3} M PA, (c) 2.0×10^{-3} M PA, (d) 0.08×10^{-3} M DBS, (e) 0.15×10^{-3} M DBS and (f) 0.1×10^{-3} M PA + 0.08×10^{-3} M DBS.

4 CONCLUSIONS

The throwing power of zinc sulfate plating baths has been found to depend strongly upon the plating parameters, viz Zn^{2+} ion concentration, pH, current density, temperature and duration. The addition of PA and/or DBS into the baths greatly improves their throwing power. However, DBS has the more pronounced improving effect on the throwing power. Such improvement is attributed to the inhibitory influence of these organic compounds on the reduction of Zn^{2+} ions. The inhibition of zinc reduction is assumed to occur via adsorption of PA or DBS molecules on the cathode surface. The adsorption is found to follow a Langimur adsorption isotherm. On the other hand, the photomicrograph of the as-plated zinc examined by using SEM shows that in the presence of PA, DBS or a combination of them, fine-grained, uniform and homogeneous electrodeposits can be obtained due to the effect of these adsorbed species. Visual observation showed that grey-zinc deposits were obtained from additives-free baths. The addition of PA to the electrolyte improves the compactness and smoothness of the deposits. However, the addition of DBS enhances the brightness of the deposits. A combination between the two additives produces compact, smooth and very bright deposits. Although the inhibition of zinc reduction is assumed to occur via adsorption of PA and/or DBS on the cathode surface, a thorough examination of the individual effect of both of them would be important in future work.

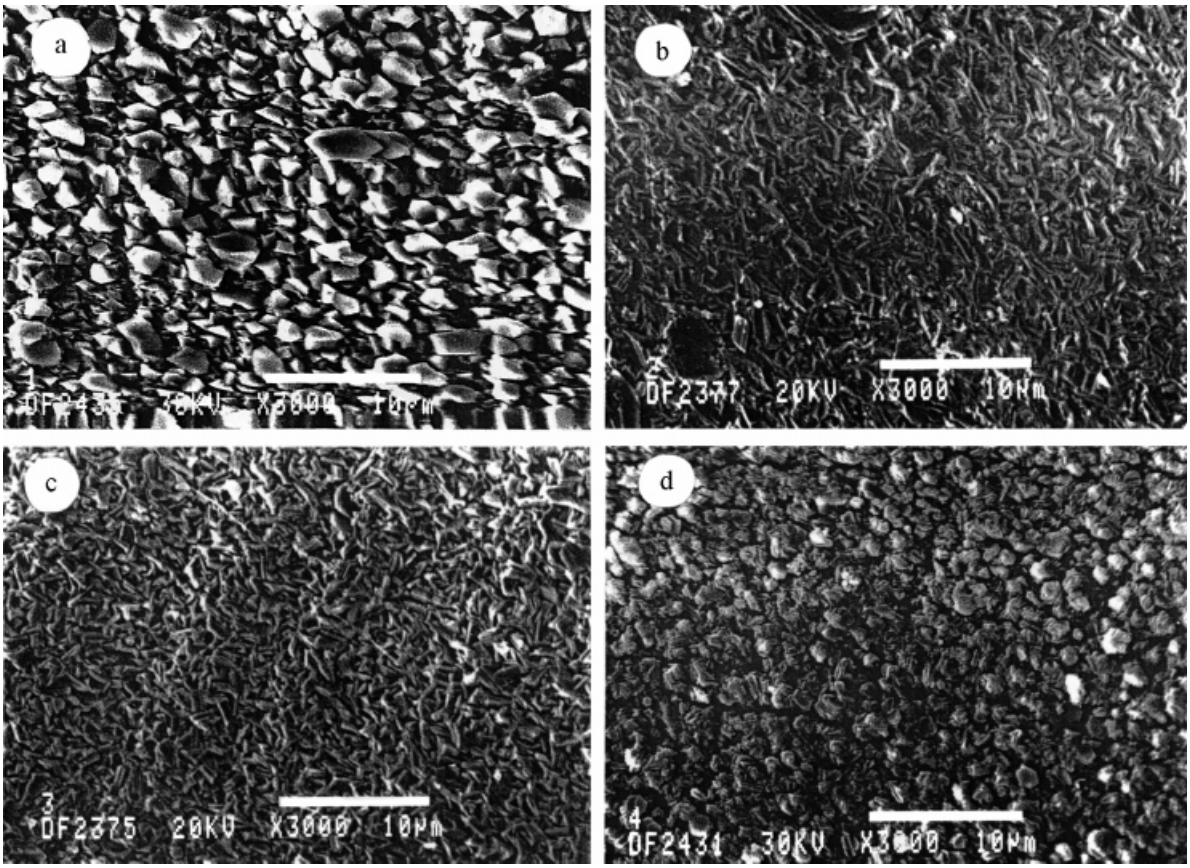

Figure 11. Photomicrographs of zinc deposited from Zn.1 bath: (a) without additive, (b) with 0.1×1^{-3}M PA, (c) with 0.08×10^{-3}M DBS, (d) with 0.1×10^{-3}M PA + 0.08×10^{-3}M DBS.

REFERENCES

1 Blum W, *Principles of Electroplating and Electroforming*, McGraw-Hill, New York (1949).

2 Zouari I and Lapicque F, An electrochemical study of zinc deposition in a sulfate medium. *Electrochim Acta* **37**:439–446 (1992).

3 Lowenheim FA, *Modern Electroplating*, 2nd edn, John Wiley & Sons, New York (1963).

4 Monev M, Mirkova L, Krastev I, Tsvetkova Hr, Rashkov St and Richtering W, Effect of brightners on hydrogen evolution during zinc electroplating from zincate electrolytes. *J Appl Electrochem* **28**:1107–1112 (1998).

5 Ambardekar DS, Anyapanawar RV and Kapadi UR, Studies on electrodeposition of zinc in ammoniacal acetate bath. *J Indian Chem Soc* **74**:334–335 (1997).

6 Abd El Rehim SS, Abd El Wahaab SM, Fouad EE and Hassan HH, Effect of some variables on the electroplating of zinc from acetate baths. *J Appl Electrochem* **24**:350–354 (1994).

7 Lin YP and Selman JR, Periodic-current—modulation effects in alkaline and acidic electrodeposition of zinc. *J Electrochem Soc* **138**:3525–3529 (1991).

8 Chandran M, Sarma RL and Krishnan RM, Zinc electrodeposition from bromide electrolytes. *Bull Electrochem* **15**:242–247 (1999).

9 Kudryavtsev N, Kuznetsov V, Nachenov G and Pachuskina L, Comparative characterization of the throwing power of copper plating electrolyte in model cells. *J Appl Chem USSR* **54**:1775–1779 (1981).

10 Kruglikov SS, Yarlkov MM, Braun EV, Klochkova MN and Savelev MI, Throwing power of a dilute copper plating bath as a function of composition. *Protection of Metals USSR* **22**:667–669 (1986).

11 Fedorova OV, Kuznetsov VV and Pashkova NM, A sulfate electrolyte with a high throwing power for copper printed circuits. *Protection of Metals USSR* **24**:399–401 (1988).

12 Kruglikov S, Yarlkov M and Yurchuk T, Influence of current reversals on the throwing power of a sulfate copper plating bath. *Soviet Electrochem* **27**:269–273 (1991).

13 Gazeeva NV, Andreev IN, Koshev AN, Samoilenko VN and Davydenko AA, Quantitative estimates of the throwing power of copper plating baths vigorously stirred and heated. *Soviet Electrochem* **28**:64–69 (1992).

14 Moshohoriton R, Tsangaraki I and Kotsira C, The effect of some additives on the throwing power and the stability of tin(II) solutions during AC coloring of anodized aluminum. *Plating and Surf Finish* **81**:53–58 (1994).

15 Abd El Rehim , Awad A and El Sayed A, The role of halides in the electroplating of tin from alkaline-stannate bath. *Surf and Coating Tech* **28**:139–143 (1986).

16 Gileadi E, Kiowa-Eisner E and Penciner P, *Interfacial Electrochemistry An Experimental Approach*, Addison-Wesley Inc Can, Reading, Massachusetts (1975).

17 Altmayer F, Fume suppression. *Plating and Surf Finish* **85**:82–84 (1998).

18 Field S, Quantitative throwing power. *Metal Ind (London)* **44**:614–617 (1934).

19 Jelinek RV and David HF, Throwing index – A new graphical method for expressing results of throwing power measurements. *J Electrochem Soc* **104**:279–281 (1957).

20 Abd El Rehim SS, Effect of superimposed AC on the electrode potential of lead in sulfuric acid solution. *Acta Chim Acad Sci Hung* **99**:289–292 (1979).

21 Abd El Rehim SS, Awad A and El Sayed A, Electroplating of antimony and antimony–tin alloys. *J Appl Electrochem* **17**:156–164 (1987).

22 Abd El Rehim SS, Abd El Wahaab SM, Ibrahim MAM and

Dankaria MM, Electroplating of cobalt from aqueous citrate baths. *J Chem Technol Biotechnol* **73**:369–376 (1998).
23 Singh VB and Tikoo PK, Electrodeposition of ternary nickel–iron–cobalt alloy from acetate bath. *Electrochim Acta* **22**:1201–1204 (1977).
24 West JM, *Electrodeposition and Corrosion Processes*, D Van Nostrand Co Ltd, New York (1965).
25 Tripathy BC, Das SC, Hefterand GT and Singh P, Zinc electrowinning from acidic sulphate solutions. *J Appl Electrochem* **28**:915–920 (1998).
26 Villamil RFV, Corio P, Rubim JC and Agostinho SML, Effect of sodium dodecylsulfate on copper corrosion in sulfuric acid media in the absence and presence of benzotriazole. *J Electroanal Chem* **472**:112–119 (1999).
27 Skoluda P and Dutkiewicz E, Adsorption of *p*-toluenesulphonate anions at the polycrystalline gold–solution interface. *Electrochim Acta* **37**:75–79 (1992).
28 Rogers RT and Talor KJ, The reactions of coumarin, cinnamyl alcohol, butynediol and propargyl alcohol at an electrode on which nickel is depositing. *Electrochim Acta* **11**:1685–1696 (1966).
29 Zhao T and Guannan M, The adsorption and corrosion inhibition of anion surfactants on aluminum surface in hydrochloric acid. *Corrosion Science* **41**:1937–1944 (1999).
30 Gabe DR, The role of hydrogen in metal electrodeposition processes. *J Appl Electrochem* **27**:908–915 (1997).
31 Raub E and Muller K, *Fundamentals of Metal Deposition*, Elsevier, Amsterdam (1967).
32 Abd El Halim AM, Fawzy MH and Mahmoud MA, Influence of bath compositions and some operating conditions on the electroplating of cobalt from aqueous sulphate baths. *Trans-IMF* **71**:48–51 (1993).
33 Wagner C, Theoretical analysis of the current density distribution in electrolytic cells. *J Electrchem Soc* **98**:116–128 (1951).
34 Marshall SL and Wolf SK, Analysis of terminal effects in rectangular electrochemical cells. *Electrochim Acta* **43**:405–415 (1998).
35 Abd El Halim AM, Electroplating of cadmium from acidic bromide baths. *J Appl Electrochem* **14**:587–594 (1984).
36 Nakamura Y, Kaneko N, Nakamura M and Nezu H, Synergistic effects of banzalacetone and benzphenone on the electrocrystallization of tin from acid stannous sulphate solutions. *J Appl Electrochem* **24**:404–410 (1994).